Controlling the delocalization-localization transition of light via electromagnetically induced transparency

Jing Cheng
Department of Physics, South China University of Technology, Guangzhou 510640, China

Guoxiang Huang
State Key Laboratory of Precision Spectroscopy, East China Normal University, Shanghai 200062, China
(Received 11 February 2011; published 31 May 2011)

We propose a scheme to realize a transition from delocalization to localization of light waves via electromagnetically induced transparency. The system we suggested is a resonant cold atomic ensemble having N configuration, with a control field consisting of two pairs of laser beams with different cross angles, which produce an electromagnetically induced quasiperiodic waveguide (EIQPW) for the propagation of a signal field. By appropriately tuning the incommensurate rate or relative modulation strength between the two pairs of control-field components, the signal field can exhibit the delocalization-localization transition as it transports inside the atomic ensemble. The delocalization-localization transition point is determined and the propagation property of the signal field is studied in detail. Our work provides a way of realizing wave localization via atomic coherence, which is quite different from the conventional, off-resonant mechanism-based Aubry-Andre model, and the great controllability of the EIQPW also allows an easy manipulation of the delocalization-localization transition.

DOI: 10.1103/PhysRevA.83.053847 PACS number(s): 42.25.Dd, 42.50.Gy, 61.44.Fw

I. INTRODUCTION

Wave propagation in periodic and disordered structures is of great importance in the study of modern physics [1,2]. One of most interesting phenomena is the wave localization in disordered media, such as the Anderson model [3]. Detailed studies on wave localization are very fundamental and useful for understanding a large amount of physical phenomena occurring in systems ranging from superfluid helium in porous media [4], disordered superconductors [5], and light propagation in disordered materials, etc. [6]. However, in condensed-matter systems the Anderson localization itself has never been observed directly due to the existence of complicated many-body interaction and other uncontrollable effects. Instead, in recent years various engineered systems have been proposed in which transportation of particles or propagation of waves can be significantly manipulated by controllable disorder. Successful examples include sound and light waves in disordered structures [6–15], quantum chaotic systems [16], and Bose-Einstein condensates (BECs) with optical potentials [17–21].

In the original Anderson model [3], the transition from extended to localized phases is expected to occur only in three dimensions (3Ds) as the strength of disorder is above a critical value [1]. It has been shown that for low-dimensional systems, only a crossover from extended to localized phases can be observed [6,13]. But other kinds of delocalization-localization transition may occur in some one-dimensional (1D) models. A well-known example is the Aubry-Andre (AA) model [22], in which a 1D quasiperiodic potential is introduced and a delocalization-localization transition can appear. In recent years there has been renewed interest in wave propagation in quasiperiodic systems [23]. Although the quasiperiodic systems are deterministic and suffer no randomness, they actually can present localization behaviors similar as in the Anderson model, thus providing intermediate situations between ordered (e.g., periodic) and disordered systems. In recent experiments, both photonic lattices [14] and BECs [18] have been used to realize the AA model and a delocalization-localization transition has been observed.

In this work, we propose a scheme to realize a new kind of AA-like delocalization-localization transition of light waves via electromagnetically induced transparency (EIT). EIT is a destructive quantum interference effect induced by a controlling field, by which the absorption of a signal field can be largely eliminated [24]. The wave propagation in EIT systems possesses many striking features, such as the significant reduction of group velocity and the giant enhancement of Kerr nonlinearity for very weak signal field, etc. Based on these features many EIT-based applications, including high-efficient multiwave mixing [24], optical quantum memory [25], optical atomic clocks [26–28], and slow-light solitons, etc. [29–32], have been investigated. In addition, if the control field is designed to have various transverse distributions, the signal field may experience refractive index modulation, which can lead to many interesting transverse effects, such as electromagnetically induced focusing [33], grating [34], waveguide [35], self-imaging [36], and some related phenomena [37,38]. Recently, based on the study of photon scattering by a two-level emitter in 1D waveguides [39], the EIT in a 1D photonic waveguide has been studied [40].

In our proposal, the system is a cold four-level atomic system with N-configuration. The control field consists of two pairs of laser beams with different cross angles, which can produce an electromagnetically induced quasiperiodic waveguide (EIQPW) for a signal field. By suitably adjusting the incommensurate rate or the relative modulation strength between the two pairs of control-field components, it is easy to realize a transition of the signal-field eigen wave functions from delocalization to localization. Our work provides a way of

realizing light-wave localization by using atomic coherence. It is quite different from the conventional Aubry-Andre systems that are based on an off-resonant scheme [14,18]. Furthermore, because the system we suggest is a coherent, resonant one, the high degree of control over the system parameters also allows us an easy manipulation of the delocalization-localization transition.

The paper is organized as follows. In the next section we give a description of the theoretical model under study. In Sec. III, we investigate the delocalization-localization transition of the signal field by manipulating the incommensurate rate and the relative modulation strength of the control field. In the final section, a summary and a discussion of our main results are given.

II. THE MODEL

We consider a cold, resonant four-level atomic system with an N-type configuration, as shown in the left lower corner of Fig. 1, in which Ω_s, Ω_p, and Ω_c are the Rabi frequencies of signal, pump, and control fields, respectively. δ and Δ are the detunings for the transition from the state $|1\rangle$ to the state $|3\rangle$ and from the state $|2\rangle$ to the state $|4\rangle$, respectively. The signal (pump) field E_s (E_p) is incident in the medium (with length L) from the left (right)-hand side. The control field consists of two pairs of laser beams ($E_{c1}^{\pm}$ and $E_{c2}^{\pm}$) with different cross angles θ_1 and θ_2, which are used to produce two different spatial periods and create a quasiperiodically modulated susceptibility distribution, and hence the EIQPW for the signal field. We assume that the system is prepared to have the population in the atomic ground state $|1\rangle$; the signal field is weak and travels along the positive z direction; the pump field is strong enough so that it will not be depleted; the control fields are a little

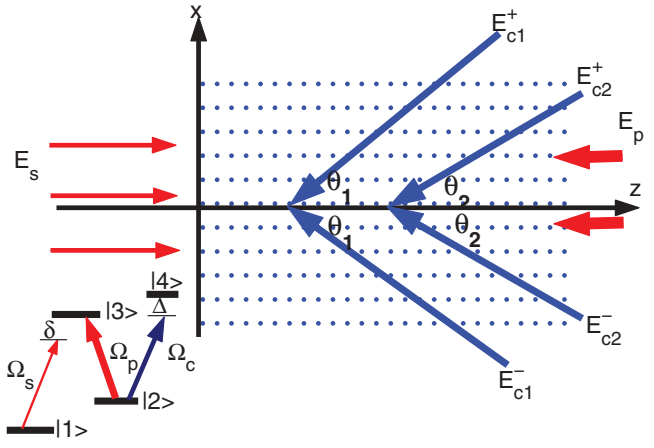

FIG. 1. (Color online) Schematic of the system for realizing the delocalization-localization transition of the signal field by using control-field-induced EIQPW. The left lower corner is the atomic energy-level configuration, in which Ω_s, Ω_p, and Ω_c are, respectively, the Rabi frequencies of signal, pump, and control fields, and δ and Δ are, respectively, detunings for the transition from the state $|1\rangle$ to the state $|3\rangle$ and from the state $|2\rangle$ to the state $|4\rangle$. The signal (pump) field E_s (E_p) is incident in the medium from the left (right)-hand side. The control field consists of two pairs of laser beams ($E_{c1}^{\pm}$ and $E_{c2}^{\pm}$) with different cross angles θ_1 and θ_2. x is the transverse coordinate and z is the coordinate along which the signal field travels.

weak but stronger than the signal field. Since the control field couples to the states $|2\rangle$ and $|4\rangle$, which always have vanishing population during the propagation of the signal field, it will also be nearly undepleted. For simplicity, we consider only one transverse dimension (with coordinate x).

The plane-wave control fields shown in Fig. 1 have the Rabi frequency $\Omega_{c1}^{\pm} = \frac{1}{2}\Omega_{c1}\exp[ik_c(\mp x\sin\theta_1 - z\cos\theta_1 \mp \psi_1)], \Omega_c^{\pm} = \frac{1}{2}\Omega_{c2}\exp[ik_c(\mp x\sin\theta_2 - z\cos\theta_2 \mp \psi_2)]$, where k_c is the wave vector, Ω_{cj} and ψ_j ($j = 1,2$) are, respectively, the amplitudes and phases of the jth component of the control field. In our studies, the cross angles are very small, $\sin\theta_{1,2} \ll 1$ and $\cos\theta_{1,2} \simeq 1$, then the transverse distribution of the control field can be written in the following form:

$$\Omega_c(x) = [\Omega_{c1}\cos(xk_c\sin\theta_1 + \psi_1) + \Omega_{c2}\cos(xk_c\sin\theta_2 + \psi_2)], \quad (1)$$

and the full control field is $\Omega_c(x)e^{-ik_cz}$. In the following, suppose $\psi_1 = \psi_2 = -\pi/2$, $\Omega_0 = \Omega_{c1}$, $\eta = \Omega_{c2}/\Omega_{c1}$, $\beta = \sin\theta_2/\sin\theta_1$, $d = (k_c\sin\theta_1)^{-1}$; we can write the standard formula of the control field used in this work,

$$\Omega_c(x) = \Omega_0\{\sin(x/d) + \eta\sin(\beta x/d)\}, \quad (2)$$

where β and η represent the incommensurate rate and relative modulation strength. This kind of field distribution is similar to the 1D incommensurate bichromatic lattice employed in the experiment of Anderson localization of BECs [18], but we shall see the difference between them soon later.

Starting from Maxwell-Bloch equations and making rotating-wave and slowly varying envelope approximations, one can obtain the equation for the envelope E of the signal field in steady state,

$$2ik_s\partial_z E + \partial_{xx}E + k_s^2\chi(x)E = 0, \quad (3)$$

where we have assumed that the signal field takes the form $\Omega_s = E(x,z)\exp[-i(\omega_s t - k_s z)]$, with $k_s = \omega_s/c$. The susceptibility $\chi(x)$ (or equivalently refractive index [42]) depends on the control field intensity $|\Omega_c(x)|^2$; its concrete expression under the EIT condition has been given in Ref. [41]. Using the scaling transform $x \sim x/(N\lambda/2\pi)$, $z \sim z/(N^2\lambda/2\pi)$ (N is a constant), Eq. (3) reduces to the standard form,

$$i\frac{\partial E}{\partial z} = -\frac{1}{2}\frac{\partial^2 E}{\partial x^2} + V(x)E, \quad (4)$$

with the effective potential $V(x) = -\chi(x)N^2/2$.

Because $\chi(x)$ is a function of $|\Omega_c(x)|^2$, it is also a quasiperiodic function of x. Thus we expect that the propagation of the signal field in the EIQPW should display a transition from delocalization to localization as shown in the AA model.

Plotted in Fig. 2 is a typical example of the control field intensity $I_c(x) \equiv |\Omega_c(x)|^2$ [Fig. 2(a)], the susceptibility function $\chi(x)$ [Fig. 2(b)], and the effective potential $V(x)$ [Fig. 2(c)]. The parameters used are atomic density $\rho = 10^{12}$ cm^{-3}, the transition dipole $\mu = 3\times10^{-29}$ m C, the decay rate of the level $|2\rangle$ $\gamma_2 = 1.5\times10^3$/s, the decay rate of the levels $|3\rangle$ and $|4\rangle$ $\gamma_{3,4} = 1.5\times10^7$/s, the signal (control) field detuning $\delta = 0$ ($\Delta = 10^9$/s), the amplitude of the Rabi frequency of the pump (control) field $\Omega_p = 10^8$/s ($\Omega_0 = 0.75\Omega_p$). The structure parameters of the control field are given by $\beta = \frac{\sqrt{5}-1}{2}$, $\eta = 0.12$, $\lambda = 780$ nm, and $N = 100$.

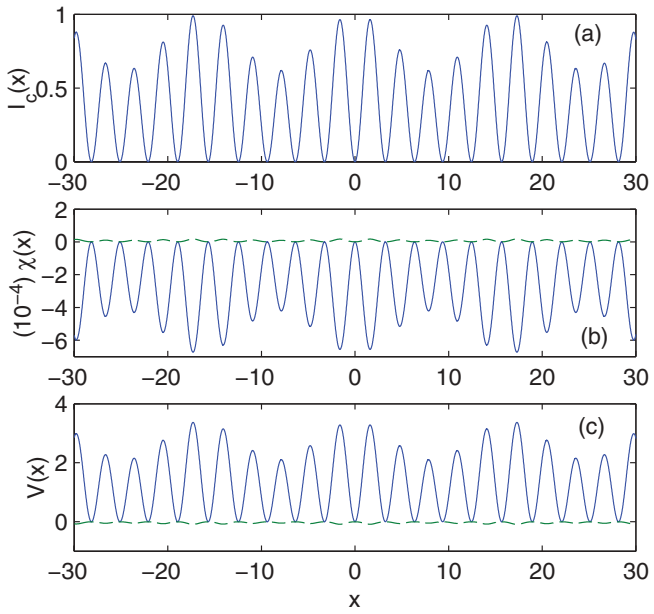

FIG. 2. (Color online) (a) Intensity distribution of the control field $I_c(x) = |\Omega_c(x)|^2$, normalized with its maximum value. (b) Profile of the susceptibility function $\chi(x)$; blue solid line denotes Re$[\chi(x)]$, green dashed line denotes Im$[\chi(x)]$. (c) The effective potential $V(x)$; blue solid line is Re$[V(x)]$, green dashed line is Im$[V(x)]$. The system parameters for plotting the figure have been given in the text.

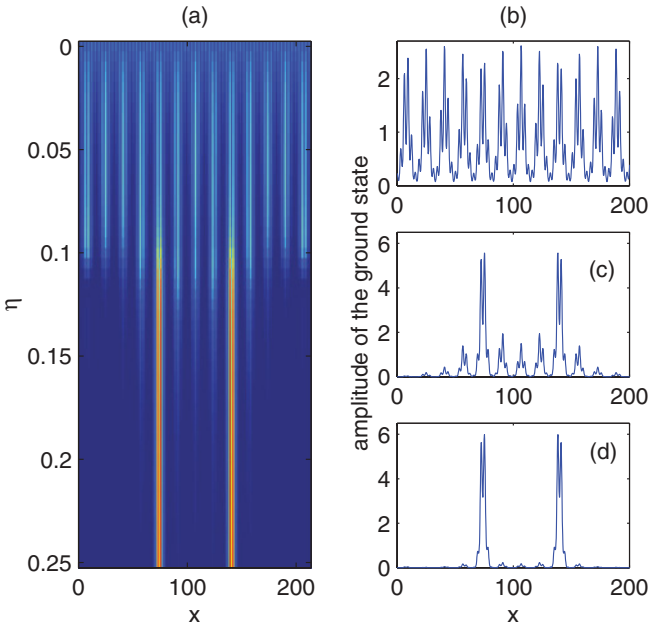

FIG. 3. (Color online) (a) Calculated amplitude profile of the ground state of the EIQPW with negligible absorption vs the transverse coordinate x and the modulation strength η. (b), (c), and (d) The amplitude of the ground state for $\eta = 0.05$, 0.12, and 0.2, respectively. Other parameters are the same as in Fig. 2.

These parameters can be realized with a cold ^{87}Rb atomic gas. From the figure we see that the effective potential $V(x)$ takes nearly the same shape as the control-field intensity $I_c(x)$. Specifically, the imaginary part of $V(x)$, i.e., Im$[V(x)]$ (green dashed line), is much smaller than its real part, i.e., Re$[V(x)]$ (blue solid line), which means that the absorption of the signal field is very small. The suppressed absorption of the signal field is due to the destructive quantum interference effect induced by the pump field [24]. A key property of our EIQPW is that all the minimum values of $V(x)$ are zero, while in the AA model, the potential minimums are quasiperiodically distributed, corresponding to quasiperiodically modulated on-site energies. Instead, in our model, the tunneling rates between neighboring potential wells are quasiperiodically modulated. However, localization transitions are still possible to occur in this model, as will be demonstrated in the following section.

III. DELOCALIZATION-LOCALIZATION TRANSITION OF THE SIGNAL FIELD

With the EIQPW designed above, we now start to investigate the delocalization-localization transition of the signal field. We first consider the ground state of the system described by Eq. (4) using numerical simulations. Notice that under the EIT condition the absorption of the system is negligible; it can thus be neglected safely in the calculation without affecting our conclusion given below. By increasing the modulation strength η from zero to large values, the effective potential $V(x)$ is found to change from periodic, to nearly periodic, and then to highly modulated quasiperiodic functions. Shown in Fig. 3(a) is the amplitude profile of the ground state presented as a function of the propagating distance x and the modulation strength η. We see clearly that when η is near zero, the ground state is extended to the whole region of x. When increasing η, the ground state becomes rugged, but it is still an extended function. However, if increasing η to a very large value, the ground state will be localized in small regions. A sharp transition is found around $\eta = 0.12$. For a better illustration, in Figs. 3(b), 3(c), and 3(d) we have plotted the amplitudes of the ground-state wave function for $\eta = 0.05$, 0.12, and 0.2, respectively. From these results we conclude that a transition from extended state to localized state of the ground-state wave function can be obtained by tuning the modulation strength η of the control-field continuously. Such tuning is easy to realize in the present-day experiment using cold atomic gases. It is interesting to note that the ground state exhibits two localized peaks for large η, as shown in Figs. 3(c) and 3(d).

The ground-state distribution presented above suggests there exists a delocalization-localization transition of the signal field in the EIQPW. Such a kind of localization transition will doubtlessly affect the propagation of the signal field significantly. To study this we consider a Gaussian distributed signal field that is initially localized tightly within a very small spatial region,

$$E(x,0) = E_0 \exp\{-x^2\}. \tag{5}$$

We simulate the propagations of this signal fields in the EIQPW numerically by using Eq. (4) with different control-field modulation strength η. The result of the amplitude distribution of the signal field $|E(x,z)|$ is presented in Fig. 4. When $\eta = 0$, the effective potential is purely periodic, and hence the signal field expands ballistically [Fig. 4(a)]. When η increases (i.e., the quasiperiodic part of the potential takes action), but below its critical value, the signal field still expands but with reduced

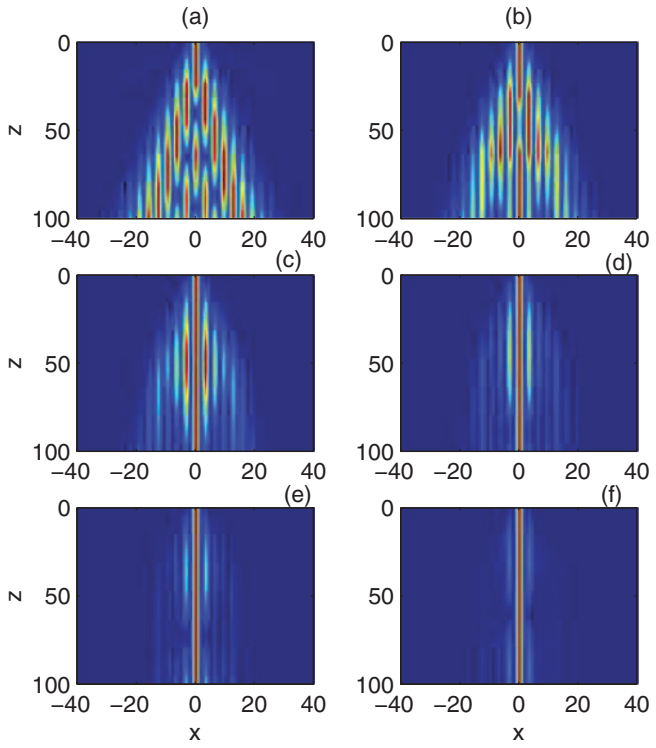

FIG. 4. (Color online) Propagation of an initially localized signal field as a function of x, z, and the control-field modulation strength η. The transverse amplitude is normalized to the corresponding maximum value at each z. Other parameters are the same as in Fig. 2. (a) $\eta = 0$, (b) $\eta = 0.04$, (c) $\eta = 0.08$, (d) $\eta = 0.12$, (e) $\eta = 0.16$, and (f) $\eta = 0.2$.

expanding rates. See Fig. 4(b) (for $\eta = 0.04$) and Fig. 4(c) (for $\eta = 0.08$). When increasing η to the value around 0.12, the signal field expands first, but the expansion stops at some distance z, i.e., it does not propagate and localizes near $x = 0$ [Fig. 4(d)]. For larger η, as depicted in Fig. 4(e) (for $\eta = 0.16$), the signal field is highly localized with a small spatial width. When η increases to 0.2, the signal field experiences only very small distortion, corresponding to a nearly perfect localization. Notice that since the initial wave packet (5) used in the simulation is not exactly the ground state of Eq. (4), some small side lobes appear in the localized signal fields.

The width of the signal-field wave packet during propagation in the EIQPW can be quantitatively characterized by the participation ratio (PR), defined by [14]

$$\mathrm{PR} = \frac{(\int |E(x,z)|^2 dx)^2}{\int |E(x,z)|^4 dx}, \tag{6}$$

which is a function of the propagation distance z and the modulation strength η. Shown in Fig. 5(a) is a 3D plot of the PR. We see clearly that for small η the value of PR increases almost linearly during the propagation of the signal field. For intermediate value of η, the PR first grows to a very large value, then it decreases gradually. When η is large enough, PR is slightly oscillated around its small initial value. The localization transition can be identified more clearly from Fig. 5(b), in which PR as a function of η for five propagation

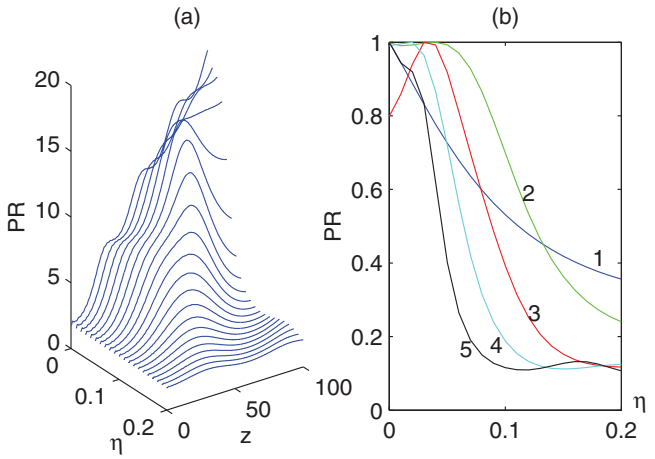

FIG. 5. (Color online) (a) 3D plot of the participation ratio (PR) as a function of the modulation strength η and propagation distance z. (b) PR as a function of the modulation ratio η for five different propagation distances $z = 20$ (blue, curve 1), 40 (green, curve 2), 60 (red, curve 3), 80 (cyan, curve 4), and 100 (black, curve 5). Each curve is normalized between 0 and 1.

distances, i.e., $z = 20$ (blue, curve 1), 40 (green, curve 2), 60 (red, curve 3), 80 (cyan, curve 4), and 100 (purple, curve 5), is presented. We see that the localization transition is sharper for larger distances.

Because our system has a high degree of control over the system parameters, which provides us an opportunity to manipulate the delocalization-localization transition conveniently. In the consideration given above the incommensurate rate β is chosen to be the golden mean ($\beta = \frac{\sqrt{5}-1}{2}$), which is the typical value in the AA model. What will happen for the delocalization-localization transition in our EIQPW for different β? To answer this, we make a new simulation with a new incommensurate rate $\beta = 0.83$. The result is provided in Fig. 6. Panels (a)–(e) of the figure are for the control-field modulation strength $\eta = 0.04$, 0.08, 0.12, 0.16, and 0.2, respectively. Panel (f) is the participation ratio as a function of z for $\eta = 0.04$ (blue, curve 1), 0.08 (green, curve 2), 0.12 (red, curve 3), 0.16 (cyan, curve 4), and 0.2 (purple, curve 5), respectively. From the figure, we see that the amplitude distribution of the signal field may still be localized, but with increased widths and side lobes, in comparison with Figs. 4 and 5. In particular, for $\eta = 0.2$ the PR increases first and then changes slightly around 5.0; but for the golden mean $\beta = \frac{\sqrt{5}-1}{2}$ the corresponding PR is oscillated around 2.0. Consequently, the incommensurate rate β can be used to significantly adjusting the degree of localization in the system.

Shown in Fig. 7(a) is a 3D plot of participation ratio as a function of β and propagation distances z. The modulation strength of the control field is fixed to $\eta = 0.2$. Other system parameters are the same as in Fig. 2. The panel (b) of the figure is the PR as a function of β for five different propagation distances, i.e., $z = 20$ (blue, curve 1), 40 (green, curve 2), 60 (red, curve 3), 80 (cyan, curve 4), and 100 (black, curve 5). Each curve in the figure is normalized between 0 and 1. We see that for large β, the PR grows as z increases; but for small β, PR remains small and only changes slightly around its initial

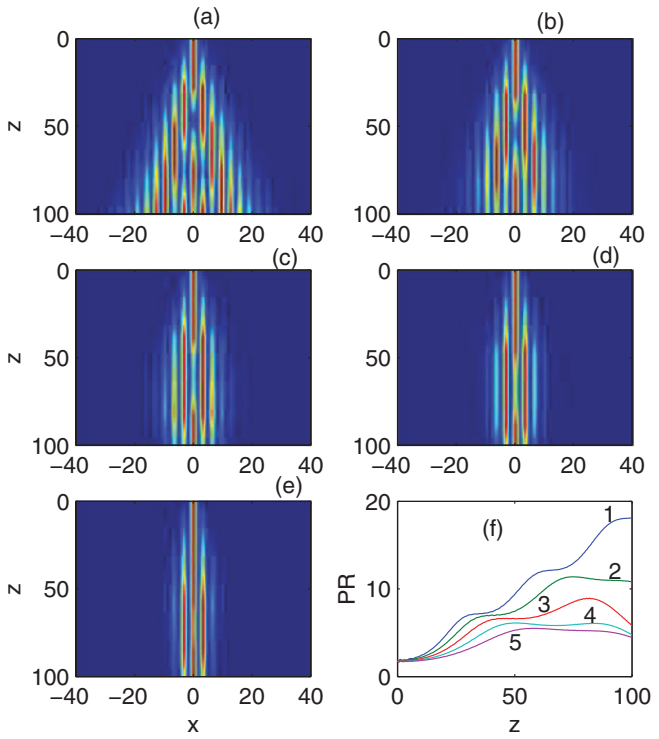

FIG. 6. (Color online) Propagation of signal field for the incommensurate rate $\beta = 0.83$. Panels (a)–(e) are for the control-field modulation strength $\eta = 0.04, 0.08, 0.12, 0.16$, and 0.2, respectively. Other system parameters are the same as in Fig. 2. The transverse amplitude of the signal field is normalized to its maximum value at each z. Panel (f) is the participation ratio (PR) as a function of z for $\eta = 0.04$ (blue, curve 1), 0.08 (green, curve 2), 0.12 (red, curve 3), 0.16 (cyan, curve 4), and 0.2 (purple, curve 5), respectively.

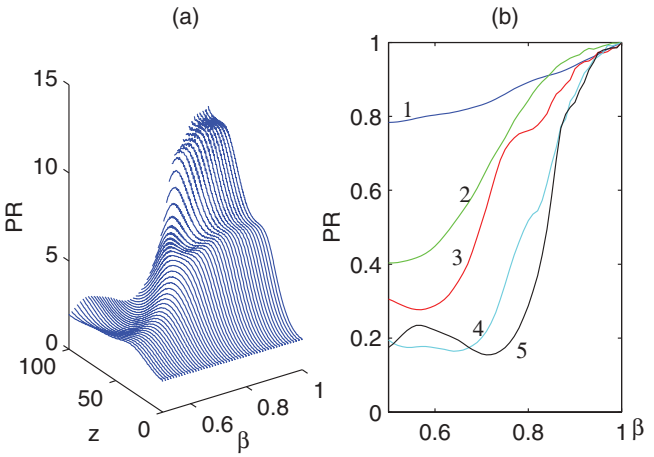

FIG. 7. (Color online) (a) 3D plot of participation ratio (PR) as a function of β and propagation distances z. The modulation strength of the control field is fixed to $\eta = 0.2$. Other system parameters are the same as in Fig. 2. (b) PR as a function of β for five different propagation distances, i.e., $z = 20$ (blue, curve 1), 40 (green, curve 2), 60 (red, curve 3), 80 (cyan, curve 4), 100 (black, curve 5). Each curve is normalized between 0 and 1.

value. The result in Fig. 7(b) shows that a sharp localization transition will occur for $\beta = 0.75$ at $z = 100$. Thus we see that when fixing the control-field modulation strength η, the delocalization-localization transition can also be observed via varying the incommensurate rate β of the EIQPW.

IV. DISCUSSION AND SUMMARY

Note that the present work is based on a quasiperiodic model, which is deterministic and has no randomness. It is close to the AA model and very different from the Anderson model. It is possible to use the EIT technique to realize the Anderson model, in which the disorder can be induced by taking optical speckles [17] as control fields. In addition, our work can be easily extended to 2D cases. There are two possible generalizations. One is to use another two pairs of control fields [similar to Eq. (2)] to generate a quasiperiodic distribution in the y direction, so that one has 2D control-field distribution:

$$\Omega_c(x,y) = \Omega_x\{\sin(x/d_x) + \eta_x \sin(\beta_x x/d_x)\} + \Omega_y\{\sin(y/d_y) + \eta_y \sin(\beta_y y/d_y)\}. \quad (7)$$

In this case of separable $\Omega_c(x,y)$, besides the localization-delocalization transition, it is possible to have localization in one direction and delocalization in the other direction. Other possible 2D generalization is to generate a nonseparable $\Omega_c(x,y)$ having a quasicrystal structure, such as the 2D Penrose tiling [43]. The delocalization-localization transition properties of 2D systems are very different from the 1D one, which is an interesting topic and deserves to be explored in future studies.

In summary, we have proposed a scheme to realize the delocalization-localization transition of light waves by using EIT in a cold, resonant four-level atomic system. In this system the pump field is used to suppress absorption and the control field is used to produce an electromagnetically induced quasiperiodic waveguide for the propagation of the signal field. By suitably adjusting the incommensurate rate and relative modulation strength between the two pairs of control-field components, the signal field may exhibit a clear transition from delocalization to localization as it transports inside the atomic ensemble. The transition point has been determined and the propagation property of the signal field has been investigated in detail.

We stress that the proposal for observing delocalization-localization transition of light waves presented here is based on the coherent manipulation of the prepared cold atomic medium. In such system one can easily tune the pump and control fields to actively modify the susceptibility (or refractive index) distribution (and hence the effective potential) of the signal field, which provides a flexible and controllable method to manipulate the dynamics of the signal field. In comparison with other schemes by using BECs or passive photonic waveguides, our proposal has particular advantages such as the flexible controllability and very weak signal beams. In fact, we can generate a susceptibility distribution with any shape as needed in a coherently prepared atomic medium with real-time tunability. Our work is the first step to simulate problems in condensed-matter physics via using the powerful EIT technique. In addition, from the basic physical

viewpoint we have also found a kind of wave localization model in which the on-site energies are constants and tunneling rates between neighbor sites are quasiperiodically changed, which is quite different with the familiar Aubry-Andre model and can increase our understanding on the nature of wave localization. More detailed studies, such as the inclusion of nonlinear effect, will be presented in a future work.

ACKNOWLEDGMENTS

This work was supported by the Natural Science Foundation of China under Grants No. 10774047, No. 10934011, and No. 10874043; by the Key Development Program for Basic Research of China under Grant No. 2006CB921104; by the Fundamental Research Funds from SCUT; and in part by the Open Fund from the State Key Laboratory of Precision Spectroscopy, ECNU.

[1] P. A. Lee and T. V. Ramakrishnan, Rev. Mod. Phys. **57**, 287 (1985); B. Kramer and A. MacKinnon, Rep. Prog. Phys. **56**, 1469 (1993).
[2] P. Sheng, *Introduction to Wave Scattering, Localization, and Mesoscopic Phenomena* (Springer, Berlin, 2006).
[3] P. W. Anderson, Phys. Rev. **109**, 1492 (1958).
[4] J. D. Reppy, J. Low Temp. Phys. **87**, 205 (1992).
[5] Y. Dubi, Y. Meir, and Y. Avishai, Nature **449**, 876 (2007).
[6] T. Schwartz, G. Bartal, S. Fishman, and M. Segev, Nature (London) **446**, 52 (2007).
[7] J. D. Maynard, Rev. Mod. Phys. **73**, 401 (2001).
[8] D. S. Wiersma, P. Bartolini, A. Lagendijk, and R. Righini, Nature (London) **390**, 671 (1997).
[9] A. A. Chabanov, M. Stoytchev, and A. Z. Genack, Nature (London) **404**, 850 (2000).
[10] T. Pertsch, U. Peschel, J. Kobelke, K. Schuster, H. Bartelt, S. Nolte, A. Tünnermann, and F. Lederer, Phys. Rev. Lett. **93**, 053901 (2004).
[11] M. Störzer, P. Gross, C. M. Aegerter, and G. Maret, Phys. Rev. Lett. **96**, 063904 (2006).
[12] S. Longhi, Phys. Rev. A **77**, 015807 (2008).
[13] Y. Lahini, A. Avidan, F. Pozzi, M. Sorel, R. Morandotti, D. N. Christodoulides, and Y. Silberberg, Phys. Rev. Lett. **100**, 013906 (2008).
[14] Y. Lahini, R. Pugatch, F. Pozzi, M. Sorel, R. Morandotti, N. Davidson, and Y. Silberberg, Phys. Rev. Lett. **103**, 013901 (2009).
[15] Y. Lahini, Y. Bromberg, D. N. Christodoulides, and Y. Silberberg, Phys. Rev. Lett. **105**, 163905 (2010).
[16] S. Fishman, D. R. Grempel, and R. E. Prange, Phys. Rev. Lett. **49**, 509 (1982); F. L. Moore, J. C. Robinson, C. F. Bharucha, Bala Sundaram, and M. G. Raizen, *ibid.* **75**, 4598 (1995); J. Chabé, G. Lemarié, B. Grémaud, D. Delande, P. Szriftgiser, and J. C. Garreau, *ibid.* **101**, 255702 (2008).
[17] J. Billy, V. Josse, Z. Zuo, A. Bernard, B. Hambrecht, P. Lugan, D. Clément, L. Sanchez-Palencia, P. Bouyer, and A. Aspect, Nature (London) **453**, 891 (2008).
[18] G. Roati, C. D'Errico, L. Fallani, M. Fattori, C. Fort, M. Zaccanti, G. Modugno, M. Modugno, and M. Inguscio, Nature (London) **453**, 895 (2008).
[19] L. Sanchez-Palencia and M. Lewenstein, Nat. Phys. **6**, 87 (2010).
[20] G. Modugno, Rep. Prog. Phys. **73**, 102401 (2010).
[21] B. Deissler, M. Zaccanti, G. Roati, C. DErrico, M. Fattori, M. Modugno, G. Modugno, and M. Inguscio, Nat. Phys. **6**, 354 (2010).
[22] S. Aubry and G. Andre, Ann. Isr. Phys. Soc. **3**, 133 (1980).
[23] G. Roux, T. Barthel, I. P. McCulloch, C. Kollath, U. Schollwock, and T. Giamarchi, Phys. Rev. A **78**, 023628 (2008); J. Biddle, D. J. Priour, B. Wang, and S. Das Sarma, e-print arXiv:1008.0361 (2010); M. Larcher, M. Modugno, and F. Dalfovo, e-print arXiv:1010.3093 (2010).
[24] S. E. Harris, Phys. Today **50**, 36 (1997); M. Fleischhauer, A. Imamoglu, and J. P. Marangos, Rev. Mod. Phys. **77**, 633 (2005).
[25] A. I. Lvovsky, B. C. Sanders, and W. Tittel, Nat. Photon. **3**, 706 (2009), and references therein.
[26] R. Santra, E. Arimondo, T. Ido, C. H. Greene, and J. Ye, Phys. Rev. Lett. **94**, 173002 (2005).
[27] T. Zanon-Willette, A. D. Ludlow, S. Blatt, M. M. Boyd, E. Arimondo, and J. Ye, Phys. Rev. Lett. **97**, 233001 (2006).
[28] T. Hong, C. Cramer, W. Nagourney, and E. N. Fortson, Phys. Rev. Lett. **94**, 050801 (2005).
[29] Y. Wu and L. Deng, Phys. Rev. Lett. **93**, 143904 (2004).
[30] G. Huang, L. Deng, and M. G. Payne, Phys. Rev. E **72**, 016617 (2005).
[31] H. Michinel, M. J. Paz-Alonso, and V. M. Pérez-García, Phys. Rev. Lett. **96**, 023903 (2006).
[32] C. Hang, V. V. Konotop, and G. Huang, Phys. Rev. A **79**, 033826 (2009).
[33] R. R. Moseley, S. Shepherd, D. J. Fulton, B. D. Sinclair, and M. H. Dunn, Phys. Rev. A **53**, 408 (1996).
[34] H. Y. Ling, Y. Q. Li, and M. Xiao, Phys. Rev. A **57**, 1338 (1998).
[35] H. Shpaisman, A. D. Wilson-Gordon, and H. Friedmann, Phys. Rev. A **71**, 043812 (2005).
[36] J. Cheng and S. S. Han, Opt. Lett. **32**, 1162 (2007).
[37] J. Cheng, S. S. Han, and Y. J. Yan, Phys. Rev. A **72**, 021801(R) (2005); J. Cheng and S. S. Han, *ibid.* **76**, 023826 (2007).
[38] J. Cheng and S. S. Han, Phys. Rev. A **73**, 063803 (2006).
[39] J.-T. Shen and S. Fan, Opt. Lett. **30**, 2001 (2005); Phys. Rev. Lett. **98**, 153003 (2007); D. E. Chang, A. S. Sorensen, E. A. Demler, and M. D. Lukin, Nat. Phys. **3**, 807 (2007).
[40] D. Witthaut and A. S. Sorensen, New J. Phys. **12**, 043052 (2010); D. Roy, Phys. Rev. Lett. **106**, 053601 (2011).
[41] S. E. Harris and Y. Yamamoto, Phys. Rev. Lett. **81**, 3611 (1998).
[42] The refractive index of the signal field is given by $n(x) = \sqrt{1+\chi(x)} \approx 1 + \chi(x)/2$.
[43] W. Steurer and D. Sutter-Widmer, J. Phys. D **41**, R229 (2007).